

**UC Berkeley**  
**SEMM Reports Series**

**Title**

Progress Report -- Behavior of Prestressed Concrete Beams at Transfer

**Permalink**

<https://escholarship.org/uc/item/3mr6g5fb>

**Authors**

Lin, Tung-Yen

Scordelis, Alex

May, H.

**Publication Date**

1956-11-01



H.D. Eberhart

**THIS REPORT IS AVAILABLE FROM:**

**NISEE/COMPUTER APPLICATIONS  
379 DAVIS HALL  
UNIVERSITY OF CALIFORNIA  
BERKELEY CA 94720**

**(415) 642-5113**

NISEE/COMPUTER APPLICATIONS  
DAVIS HALL  
UNIVERSITY OF CALIFORNIA  
BERKELEY, CALIFORNIA 94720  
(415) 642-5113

SESM 56/02

**SERIES 100  
ISSUE 2**

**STRUCTURES AND MATERIALS RESEARCH  
DIVISION OF CIVIL ENGINEERING**

---

---

# **PROGRESS REPORT BEHAVIOR OF PRESTRESSED CONCRETE BEAMS AT TRANSFER**

**BY  
T. Y. LIN  
A. C. SCORDELIS  
H. MAY**

---

---

**NOVEMBER 1956**

**INSTITUTE OF ENGINEERING RESEARCH  
UNIVERSITY OF CALIFORNIA  
BERKELEY CALIFORNIA**



PROGRESS REPORT — BEHAVIOR OF PRESTRESSED

CONCRETE BEAMS AT TRANSFER

Sponsor: Division of Architecture, State of California

Faculty Investigators: T. Y. Lin  
A. C. Scordelis

Research Engineer: H. May

November 1956  
University of California  
Berkeley 4, California

## INTRODUCTION

This progress report presents the results of tests on three concrete beams, of rectangular cross section, subjected to eccentric prestress and external negative moment. The beams were tested to ultimate failure. These three beams are part of an overall program embodying a total of eighteen beams.

It is the purpose of this report to indicate the analytical procedure being used to derive a theory for predicting the behavior of beams under these effects and also to describe the experimental procedure used in the tests to verify the theory.

## OBJECTIVES

The main objective of this project is to determine the behavior of concrete beams and slabs under the action of eccentric prestressing. Present practice bases the design at transfer on an allowable amount of tensile stress or in some cases no tensile stress at all, although it is known that such arbitrary rules yield divergent factors of safety, varying perhaps from 1 to 4. This project is designed to include the effect of the following variables on the strength and deflection of beams and slabs at transfer:

1. The shape of cross-section - rectangular or T-shape.
2. The amount of external moment - acting to increase the eccentricity of prestress.
3. The amount of mild steel on the tensile side.

The over-all testing program will investigate the effect of these variables by testing eighteen beams. Three different shapes will be used, one rectangular and two T shapes, to investigate the effect of variable 1. Each specimen will be subjected to varying

combinations of prestress and external moment to note the effect of variable 2. Approximately half of the beams will be tested without mild steel and half with mild steel to investigate the effect of variable 3.

Up to the present time three beams of the same rectangular cross section, without mild steel, subjected to varying combinations of prestress and external moment have been tested.

#### DESCRIPTION OF TEST BEAMS (see figure 1)

The beams, all identical, had a uniform 6 inch x 20 inch rectangular cross-section over their 20 foot length. Each beam contained one prestressing cable, which consisted of 12 wires of 1/4 inch diameter with cold-formed buttons at the ends of the wires. The wires were greased and wrapped with paper and were anchored to the concrete with "General Prestressing" anchorages. Over-all diameter of the cable was approximately 1 inch.

The cable profile was parabolic in the center 4 foot portion of the beam and thence straight to each end of the beam. The cable was located at mid-depth at each end of the beam and dropped to 8 inches below mid-depth at the mid span cross-section, Fig. 1.

Beams were cast in wooden forms coated with "C.P. Bond Breaker". Five-sixteenth inch rods placed horizontally through the side forms held the cable in its correct profile during casting. These rods were removed about 4 hours after casting. The holes left by the rods were not grouted. Wire ties were used to hold the cable in its correct horizontal alignment.

The forms were stripped 3 to 7 days after casting. The specimens were cured moist for 7 days using damp burlap and then left air dry until testing at the age of 14 days.

## MATERIALS

The concrete for the beams was designed to possess a minimum strength of 4500 psi at 14 days, using 6 x 12 cylinders. The concrete was mixed in a 2.5 cubic foot mixer, eight and one half batches being necessary to cast each beam and corresponding control specimens. The mix, identical for the three beams, contained 7 sacks of Santa Cruz, Type 1, cement per cu. yd. of concrete. The water cement ratio was 5 gallons per sack. The aggregate consisted of Elliot S. E. Sand and Elliot 3/4 in. gravel. Mix proportions were 1:1.78; 2.93 by weight. Slump varied between 2.3 in. and 2.7 in.

Control specimens consisted of a minimum of three 6 x 12 in. cylinders and three 6 x 6 x 20 in. beams for each test. All control specimens were cured in the same manner as the test beams and tested at 14 days. Average values for compressive strength and modulus of elasticity obtained from the cylinders and modulus of rupture obtained from the control beams are tabulated below. A typical stress strain diagram for a 6 x 12 cylinder is shown in Figure 2.

Test Specimen	B-1A	B-1B	B-1C
Average Compressive strength of 6 x 12 in. cylinders, psi	4901	5492	4724
Secant modulus of elasticity, at 1000 psi, of 6 x 12 in. cylinders, psi	$3.23 \times 10^6$	$3.29 \times 10^6$	$3.18 \times 10^6$
Modulus of rupture of 6 x 6 x 20 in. beams on 18 in. span under third point loading, psi	530	602	488

The prestressing cables each contained 12 - 1/4 in. diameter cold drawn steel wires. The wire possessed an ultimate strength of 252,000 psi, with a proportional limit of 160,000 psi, and a yield point of 230,000 psi, as measured by the 0.2 percent offset method.

Total elongation was 2.2 percent in a gage length of 10 in. The modulus of elasticity was  $27 \times 10^6$  psi up to the proportional limit. A typical stress strain curve is shown in Figure 3.

#### METHOD OF LOADING AND INSTRUMENTATION

It was desired to have a method of loading which could apply to the critical center section of beam varying amounts of prestress force  $F$ , and external negative moment,  $M$ . The loading arrangement shown in Figure 4 was used to accomplish this purpose.

The amount of prestressing force was controlled by a hydraulic jack at one end. The value of the force was determined from a pressure gage, connected to the jack, which had been previously calibrated. From earlier pilot tests in the laboratory the friction loss in the cable to the center of beam was known to be approximately 5% and this factor was used to determine the prestress force existing at the center cross-section. The amount of external negative moment was controlled by adding weights to the ends of overhanging steel loading beams.

Instrumentation was designed so as to measure strain distribution at the center cross-section and deflections at the center and two ends of the beam.

Strains were measured by means of SR 4, type A9, strain gages which have a gage length of six inches. Eight of these gages were employed for each beam, all at the center cross-section and located as shown in Figure 5. Gages 1, 4, 5, 6, 7, 8 were connected to a Sanborn Recorder which gave a continuous automatic reading on paper of the strain as the test progressed. Gages 4 and 5 and gages 6 and 7 were wired in parallel so that an average value for strain at these levels was recorded. Gages 2 and 3 were read independently by means of standard SR-4 strain indicator box. These values were read after each

load increment had been applied until tension cracks in the beam made them inoperative. All SR-4 gages were bonded to the beam using standard procedures. Deflections were measured by simple dial gages bearing on the top of the beam. The dials had a least count of 0.001 inch.

#### THEORETICAL STUDIES

The theory which the first three beam tests sought to verify, can be easily derived since the rectangular cross-section without mild steel in the top is a simple case to investigate. However, these beams give an excellent opportunity to visualize the general behavior of beams under these loading conditions.

The following assumptions are made:

1. Plane sections remain plane after bending occurs.
2. The actual stress-strain curve for the concrete is replaced by the curve shown in Figure 6. This curve is based on the well known Jensen Theory for ultimate strength.<sup>1</sup>
3. The plasticity of the concrete in compression may be defined by Jensen's plasticity ratio

$$\beta = \frac{1}{1 + \left[ \frac{f'_c}{4000} \right]^2}$$

4. The concrete has a specified tensile strength, up to and through the cracking range, but it's contribution to the

1. "The Plasticity Ratio of Concrete and its Effect on the Ultimate Strength of Beams". by V. P. Jensen, Journal of ACI Vol. 39.



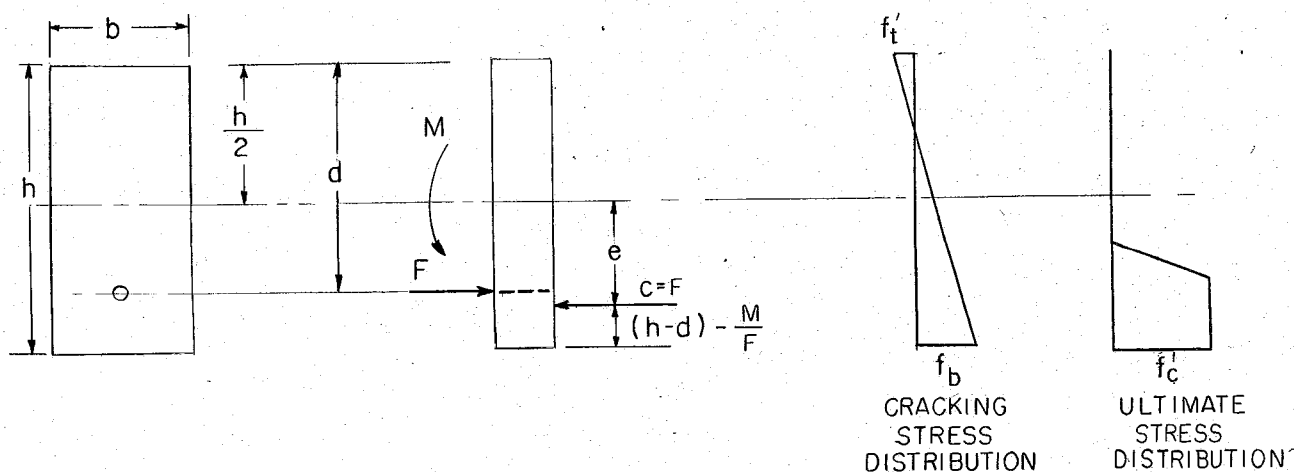
ultimate strength is neglected because it is small.

5. The effect of a prestress force  $F$  fixed in location plus an external moment  $M$  can be replaced by an equivalent system consisting of the prestress force  $F$  alone moved through a vertical distance  $\frac{M}{F}$ .

The behavior of a beam subjected to eccentric prestress force and external negative moment may be described by noting Figure 7 and 8. (a) As  $F$  or  $M$  is increased the top fiber strain and stress increase until finally the tensile strength of the concrete  $f'_t$  is reached and an initial crack forms in the top; (b) and (c) With increasing  $F$  or  $M$  the crack progresses downward, with a corresponding downward movement of the neutral axis, until finally the bottom fiber stresses reaches  $f'_c$  and plasticity starts; (d) The plasticity of the concrete is exhausted and the concrete crushes resulting in ultimate failure.

It should be noted here that in certain cases depending on the combination of  $F$  and  $M$  existing at the critical section the ultimate strength is less than the cracking strength. In these cases once the beam has cracked at the top a sudden failure will ensue.

#### Derivation of Cracking and Ultimate Strengths



The position of the C line at any time can be specified by:

$$e = d - \frac{h}{2} + \frac{M}{F} \quad \text{-----(1)}$$

### Cracking Strength

Tensile strength of concrete =  $f'_t$

Compressive strength of concrete =  $f'_c$

Moment of inertia of gross section =  $I$

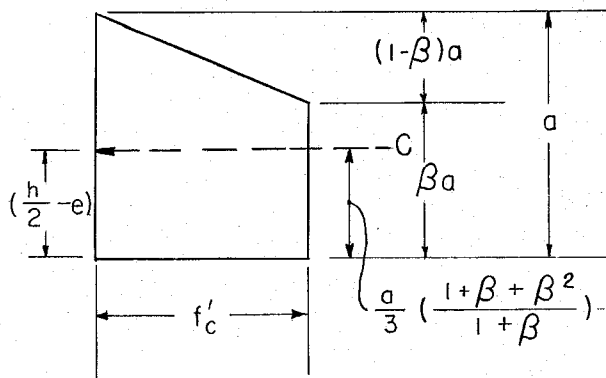
Area of gross section =  $A$

$$f'_t = - \frac{F}{A} + \frac{Feh}{2I}$$

$$= \frac{F}{A} \left[ \frac{6e}{h} - 1 \right]$$

For cracking  $\frac{F}{Af'_c} = \frac{f'_t/f'_c}{\left[ \frac{6e}{h} - 1 \right]}$  -----(2)

### Ultimate Strength



Let  $k_1 = \left( \frac{1 + \beta}{2} \right)$

$$k_2 = \left( \frac{1 + \beta + \beta^2}{1 + \beta} \right)^{\frac{1}{3}}$$

$$\Sigma H = 0$$

$$F = C = k_1 abf'_c$$

$$\Sigma M = 0$$

$$ak_2 = \left( \frac{h}{2} - e \right)$$

$$a = \frac{1}{k_2} \left( \frac{h}{2} - e \right)$$

$$F = C = k_1 \left( \frac{1}{k_2} \right) bf'_c \left( \frac{h}{2} - e \right)$$

For ultimate  $\frac{F}{Af'_c} = \frac{k_1}{k_2} \left[ \frac{1}{2} - \frac{e}{h} \right]$  -----(3)

The constants  $k_1/k_2$  are dependent on the plasticity ratio  $\beta = \frac{1}{1 + \left[ \frac{f'_c}{4000} \right]^2}$

The variation of  $k_1/k_2$  with  $f'_c$  is indicated below.

$f'_c$ psi	2000	3000	4000	5000	6000
$k_1/k_2$	1.99	1.97	1.93	1.88	1.83

For practical purposes it can be assumed a constant value of 2.0 for all strengths of concrete yielding the following equation for ultimate strength.

$$\frac{F}{Af'_c} = \left[ 1 - \frac{2e}{h} \right] \text{-----} (4)$$

It is interesting to note that the same equation is obtained using the Whitney theory for ultimate strength.

Equations (2) and (4) are represented graphically in Figure 9. It can be seen that each "cracking" curve intersects the "ultimate" curve at two locations. These two intersections in each case define the "critical eccentricity ratios". For the lower "critical eccentricity ratio" the beam will never crack, since it will fail in compression of the bottom fiber prior to the cracking load. This is a case seldom encountered in practice. For values above the higher "critical eccentricity ratio" the prestress force required to produce initial cracking is greater than that which the section can sustain at ultimate, indicating that once the section has cracked a sudden compression failure will ensue.

An equation for the "critical eccentricity" can be obtained by

equating equation (2) to equation (4).

$$\left(\frac{e}{h}\right)_c = .333 \pm \sqrt{\frac{-f'_t/f'_c + .333}{12}} \text{ ----- (5)}$$

Values of  $\left(\frac{e}{h}\right)_c$  and corresponding prestress forces  $F/Af'_c$  for various values of  $f'_t/f'_c$  are tabulated below.

$f'_t/f'_c$	.07	.08	.09	.10	.11	.12	.13
Higher $\left(\frac{e}{h}\right)_c$	.481	.479	.475	.472	.470	.466	.463
Higher $F/Af'_c$	.038	.042	.050	.056	.060	.068	.074
Lower $\left(\frac{e}{h}\right)_c$	.185	.187	.191	.194	.196	.200	.203
Lower $F/Af'_c$	.630	.626	.618	.612	.600	.608	.594

### TEST RESULTS

The three beams tested behaved essentially as predicted by the theory. The loading sequence for the first two beams, B-1A and B-1B, was selected so that the theoretical ultimate strength would be greater than the cracking strength, thus yielding a slow gradual failure. The tests of these two beams verified the expected behavior. Even though initial cracking occurred at relatively low loads the beams did not show any major signs of distress until much heavier loads had been introduced. Tensile cracks became larger and more widespread as the external loads, and therefore the external moment, were increased. Final failure occurred when the cracks had propagated down to a level where the remaining concrete section could not sustain the eccentric prestress force in compression and a final crushing of the concrete occurred. Just prior to the failure, the width of the

tensile cracks at the top of the beams measured as much as  $1/4$  in. across. The loading sequence for the third beam, B-1C, was selected so that the theoretical ultimate strength would be less than the cracking strength, thus yielding a sudden failure. The test of this beam also verified the predicted behavior in that once the beam experienced a major tensile crack it failed suddenly and completely. The loading sequence used in each of the three tests is described below. Prestress force,  $F$ , and external moment,  $M$ , indicated refer to those existing at the midspan cross-section.

B-1A a)  $M$ , 0-11.7 in. kips;  $F$ , 0

b)  $M$ , 11.7 in. kips;  $F$ , 0-40.3 kips

c)  $M$ , 11.7-70.7 in. kips;  $F = 40.3$  in kips

Initial Cracking  $F = 38.8$  kips,  $M = 11.7$  in. kips

Ultimate Failure  $F = 40.7$  kips,  $M = 70.7$  in. kips

B-1B a)  $M$ , 0-16.0 in. kips;  $F$ , 0

b)  $M$ , 16.0 in. kips;  $F$ , 0-79.3 kips

c)  $M$ , 16.0-65.4 in. kips,  $F = 79.3$  kips

Initial Cracking  $F = 34.7$  kips,  $M = 16.0$  in. kips

Ultimate Failure  $F = 79.3$  kips,  $M = 65.4$  in. kips

B-1C a)  $M$ , 0-34.8 in. kips;  $F$ , 0

b)  $M$ , 34.8 in. kips;  $F$ , 0-18.0 kips

c)  $M$ , 34.8-121.6 in. kips;  $F = 18.0$  kips

Initial Cracking  $F = 18.0$  kips,  $M = 121.6$  in. kips

Ultimate Failure  $F = 18.0$  kips,  $M = 121.6$  in. kips

A comparison between theoretical and test values is made below.

The theoretical values were obtained using equations (2), (4), and (5) together with the tensile and compressive strengths obtained from the control specimens.



				Theoretical Results				Test Results			
	$f'_t$ psi	$f'_c$ psi	A in <sup>2</sup>	$\frac{F_{crack}}{A f'_c}$	$\left(\frac{e}{h}\right)_{crack}$	$\frac{F_{ult}}{A f'_c}$	$\left(\frac{e}{h}\right)_{ult}$	$\frac{F_{crack}}{A f'_c}$	$\left(\frac{e}{h}\right)_{crack}$	$\frac{F_{ult}}{A f'_c}$	$\left(\frac{e}{h}\right)_{ult}$
B-1A	530	4901	120	.068	.432	.068	.466	.066	.415	.069	.487
B-1B	602	5492	120	.053	.510	.120	.440	.053	.423	.120	.441
B-1C	488	4724	120	.032	.736	.032	.459	.032	.740	Sudden Failure after cracking	

It can be seen from the results indicated above that the actual cracking strengths of the first two beams were slightly less than the theoretical values. Taking into account the difficulty in determining the true tensile strength of the concrete the results were considered satisfactory. The actual tensile stress in the top fiber at cracking for beam B-1A was 481 psi and for beam B-1B was 445 psi. The agreement between all other theoretical and test results is quite close.

The assumption that plane sections remain plane was verified as can be seen by the plots of strain distribution shown in Figure 10. (a) prior to cracking, (b) after cracking, (c) at ultimate. Note for B-1C, only a strain distribution just prior to cracking is shown since the beam failed suddenly after cracking.

Figures 11, 12, 13, indicate measured total deflections at the center of the beam relative to the two ends. As both prestress force and external moment produce deflections these values are both used in the ordinate axis, with the scale for each so adjusted as to give a continuous curve. The theoretical deflection curve was obtained

using the elastic theory for uncracked sections with a secant modulus of elasticity of 1000 psi, as tabulated on page 3. In Figure 14 may be seen photographs of the beam center cross-section at failure. Note the typical initial tension failure at the top, followed by a propagation of the crack downward, with a final crushing out of the concrete at the bottom.

### CONCLUSIONS

Since only 3 out of 18 specimens have been tested, definite conclusions cannot be drawn. However, in view of the close agreement between the experimental and the theoretical values, the following tentative conclusions can be advanced:

1. The cracking strength of concrete beams and slabs under excessive eccentric prestress can be determined by the usual elastic theory, using the modulus of rupture of concrete as a measure of the starting of cracks.

2. Before the cracking of the beams, the deflections under excessive eccentric prestress can be approximated by the elastic theory, using proper values of modulus of elasticity. The deflection increases more rapidly with load after the cracking of the beams.

3. For each rectangular beam, there are two "critical eccentricity ratios",  $e/h$ , a higher one and a lower one. For  $e/h$  less than the "lower critical ratio" (about 0.2), the beam will never crack, but will fail under compression when the average prestress reaches about  $0.6f'_c$ . This case is seldom encountered in practice.

4. For  $e/h$  greater than the higher critical ratio (about 0.46), compression failure will occur as soon as the beam cracks. This is

considered as very undesirable, and should be avoided in practice. This is an important finding not described in the literature.

5. For  $e/h$  between the two critical ratios (i.e. between about 0.2 and 0.46), the beam will crack first, but will not rupture completely until the load or the eccentricity or both are further increased. The factor of safety of the beam after the cracking will vary with the  $e/h$  ratio. For ratios near the critical values, the factor of safety is low.

6. The effect of externally applied moment  $M$  may be considered as equivalent to a movement of the c.g.s. through a distance equal to  $M/F$ , where  $F$  is the total prestress.

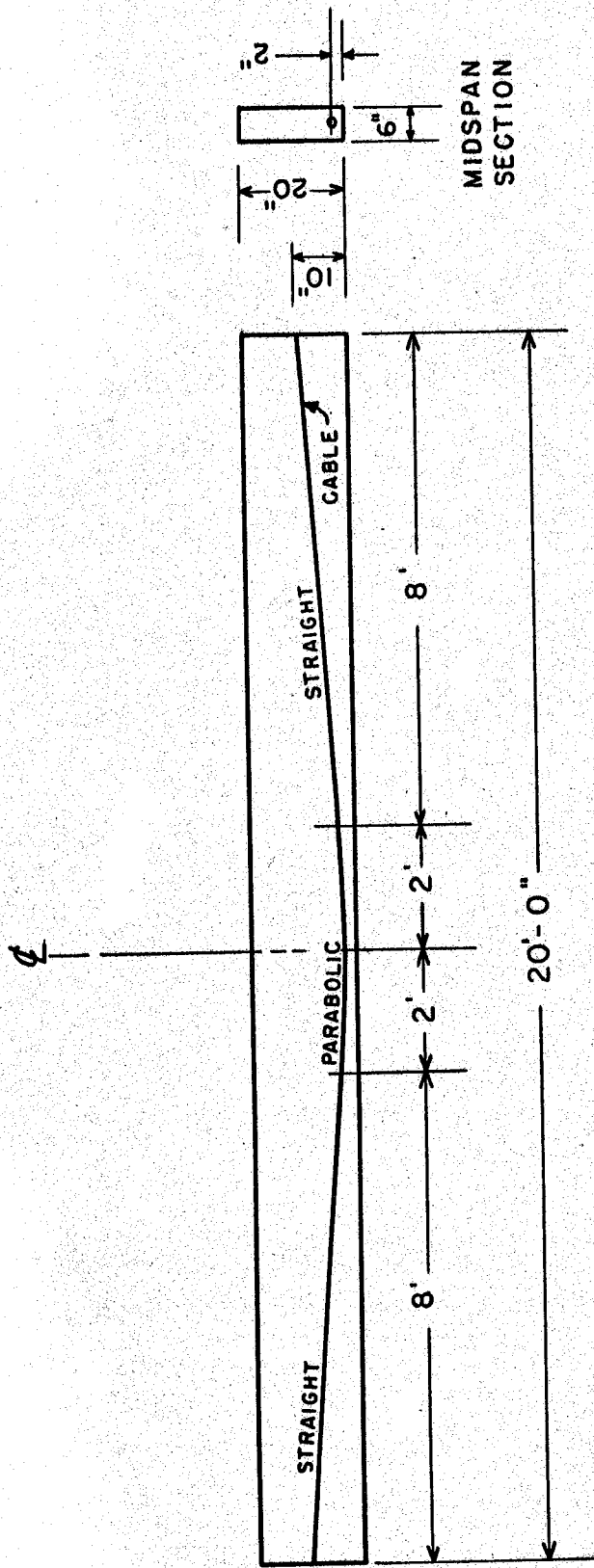


FIG. 1 BEAM LAYOUT

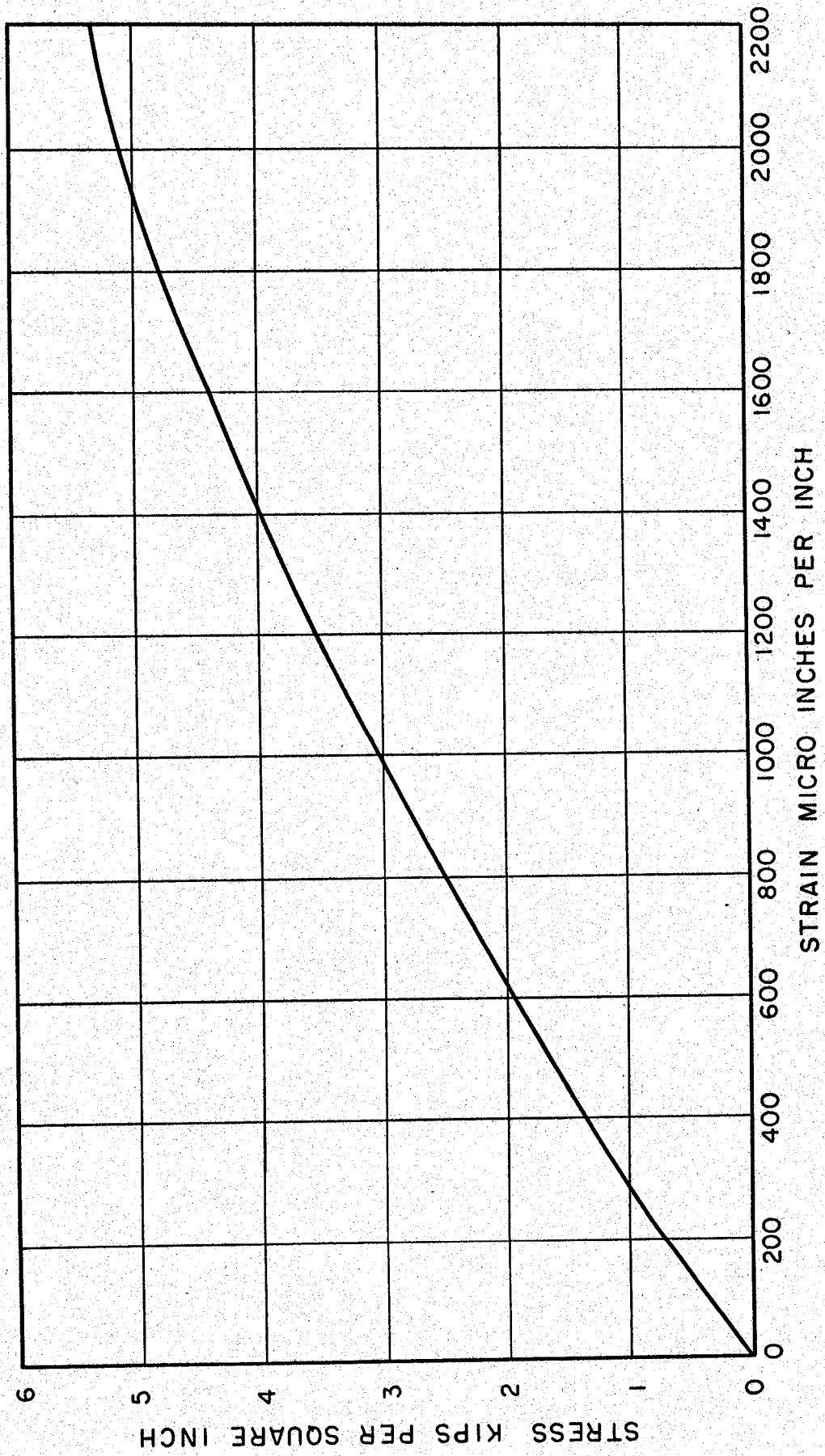


FIG. 2 TYPICAL STRESS STRAIN FOR CONCRETE. 6 x 12 IN. CYLINDER AT AGE OF 14 DAYS



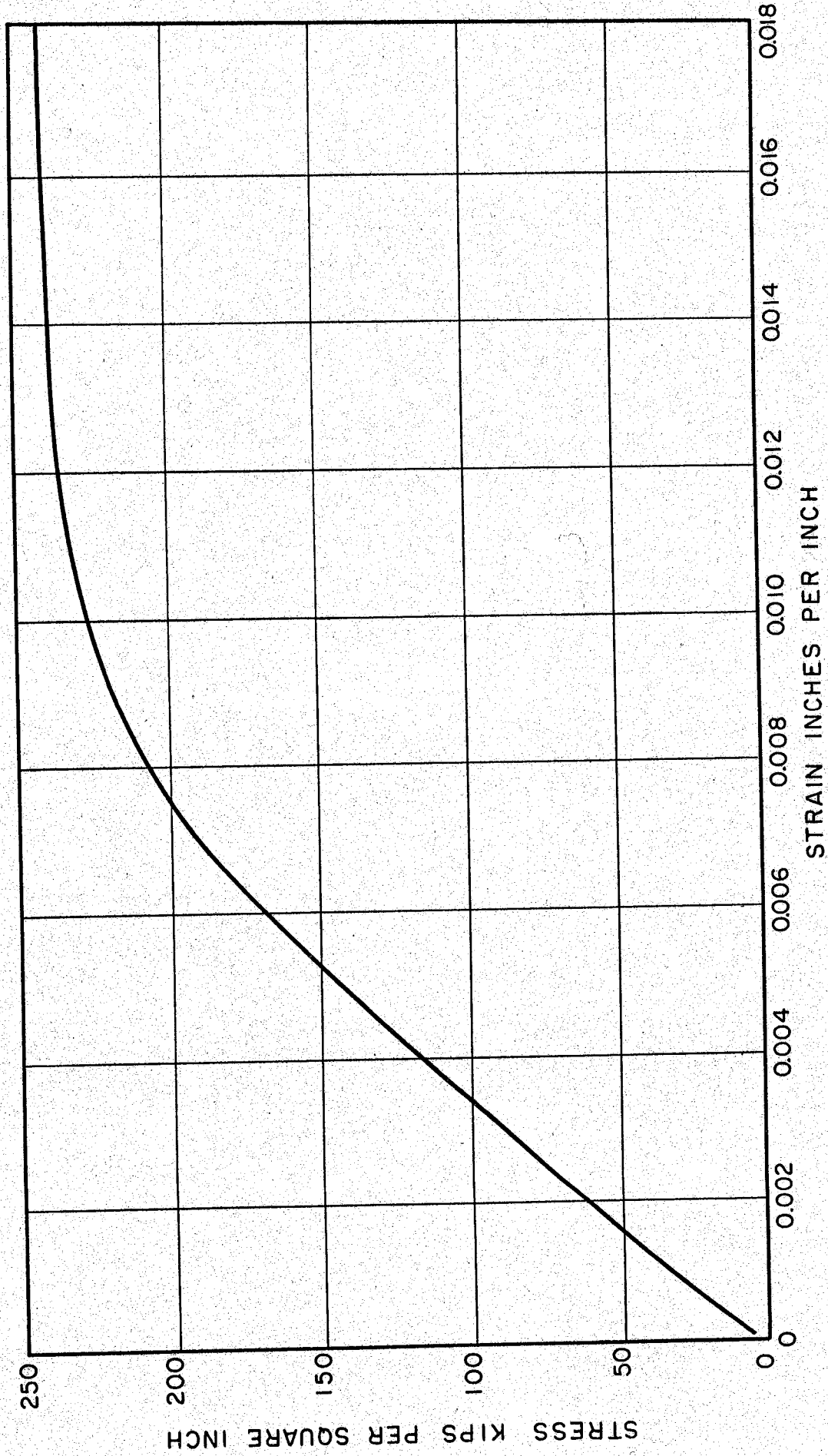


FIG. 3 TYPICAL STRESS STRAIN CURVE FOR 1/4 IN. DIA. PRESTRESSING STEEL WIRE

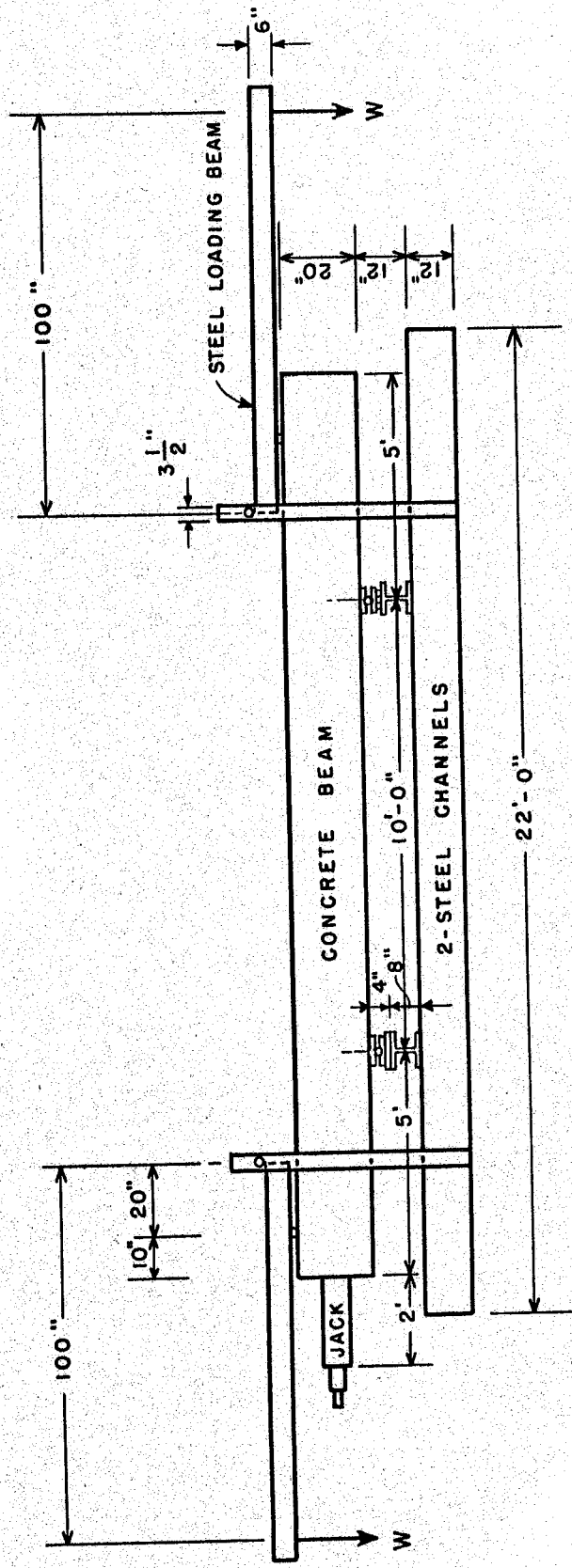


FIG. 4 LOADING ARRANGEMENT

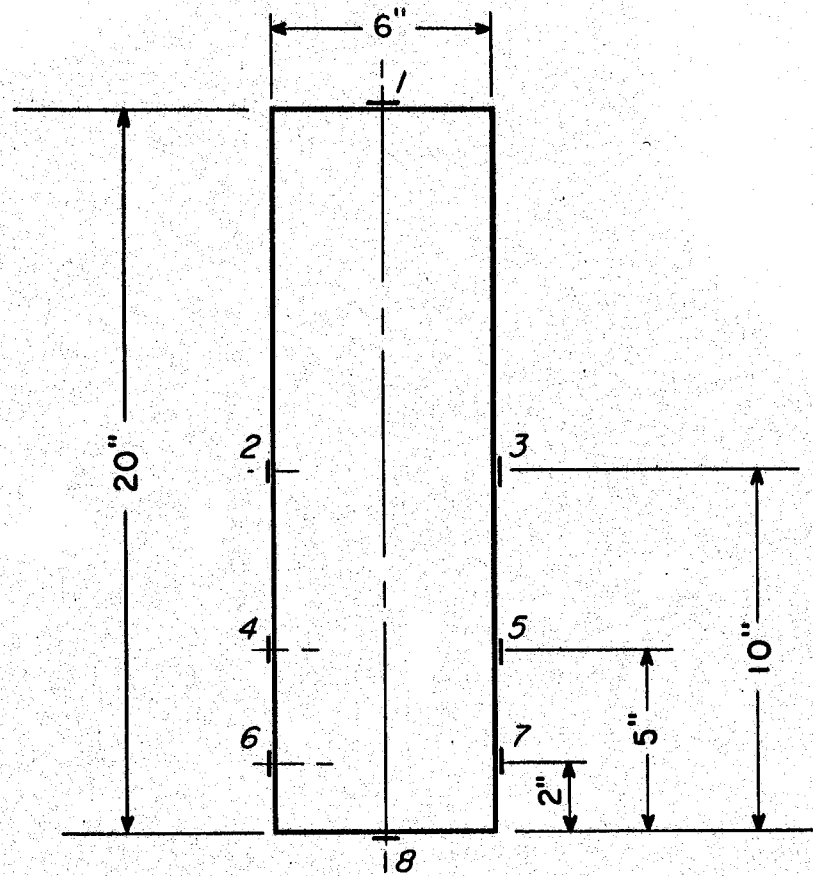


FIG. 5 LOCATION OF SR-4 GAGES AT MIDSPAN

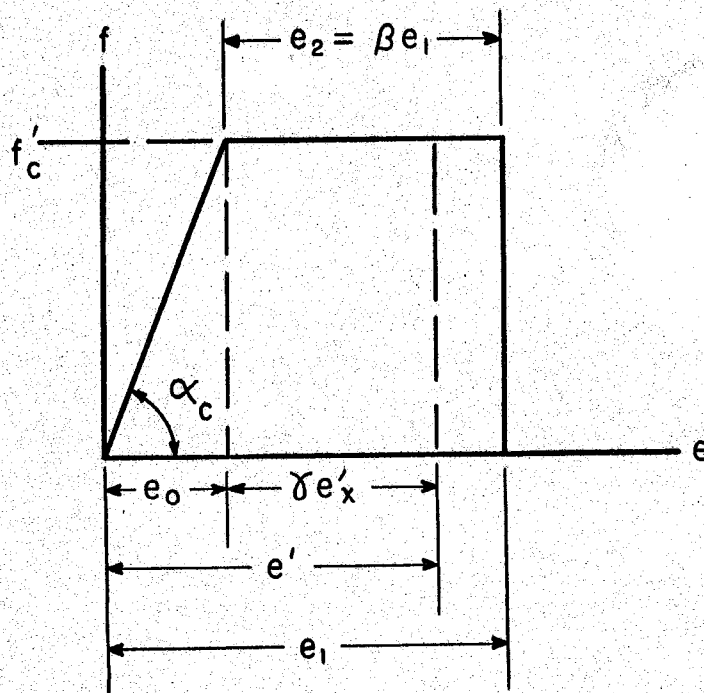


FIG. 6 ASSUMED COMPRESSIVE STRESS STRAIN CURVE BY JENSEN THEORY

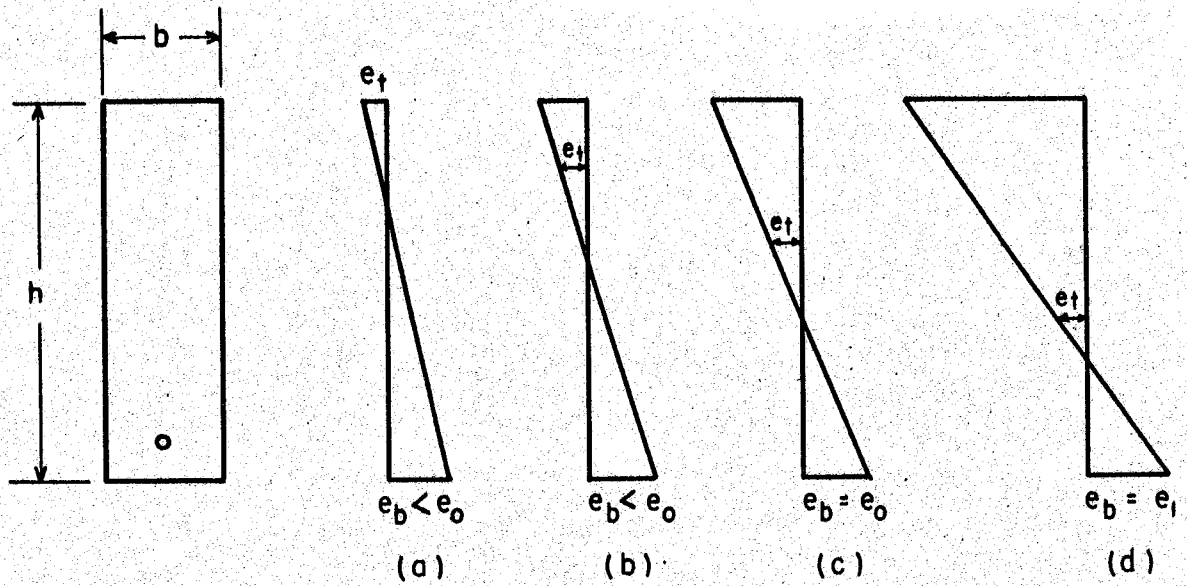


FIG. 7 STRAIN DISTRIBUTION UNDER INCREASING PRESTRESS FORCE OR EXTERNAL MOMENT

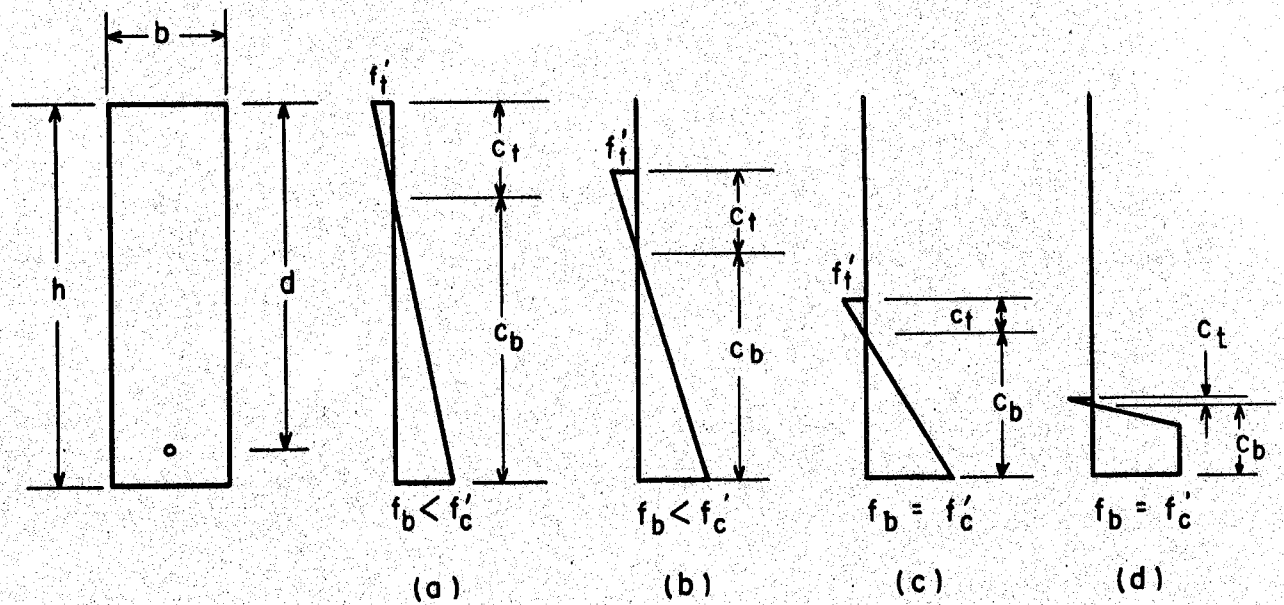


FIG. 8 STRESS DISTRIBUTION UNDER INCREASING PRESTRESS FORCE OR EXTERNAL MOMENT

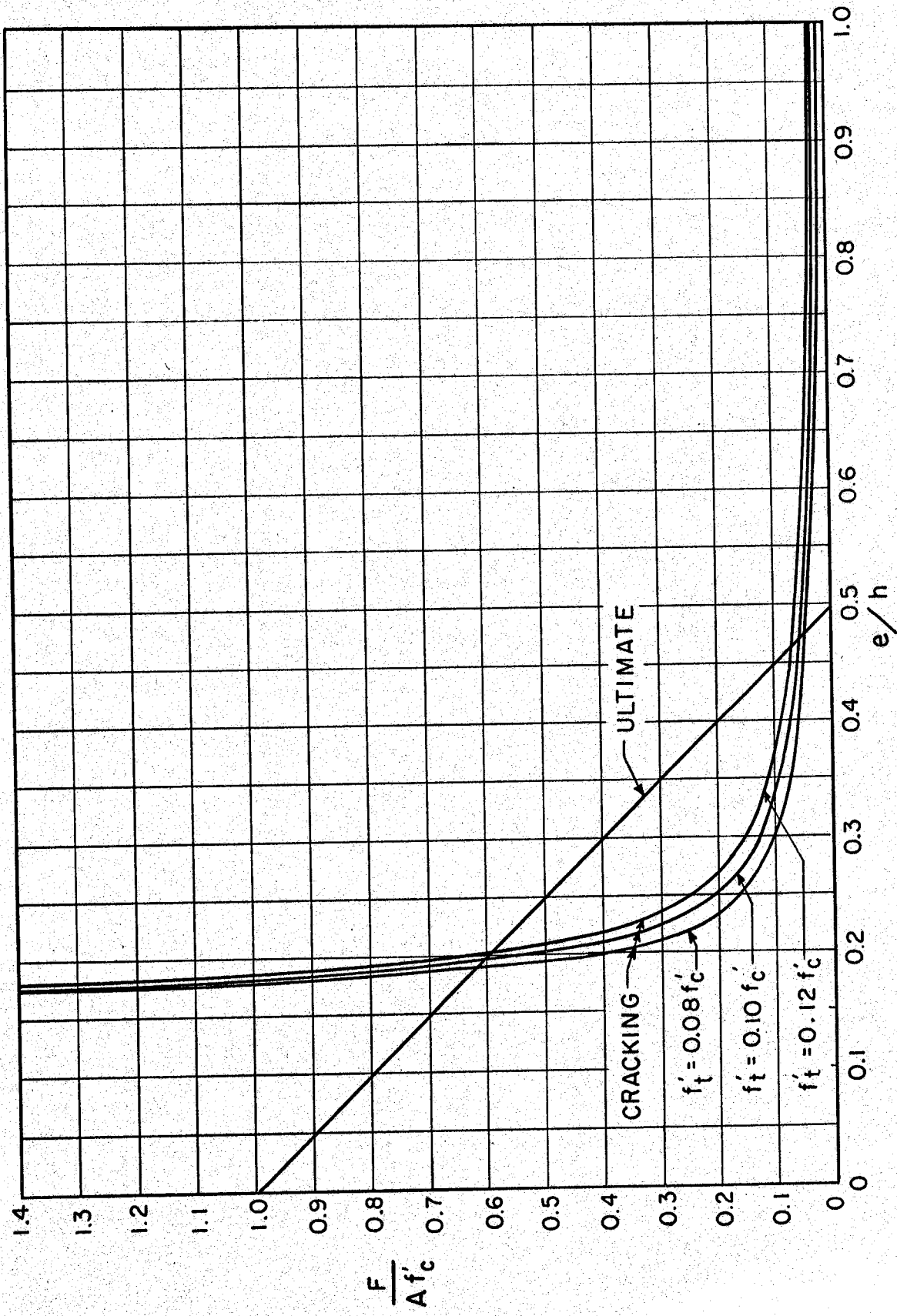


FIG. 9 CRACKING AND ULTIMATE CURVES FOR A RECTANGULAR SECTION



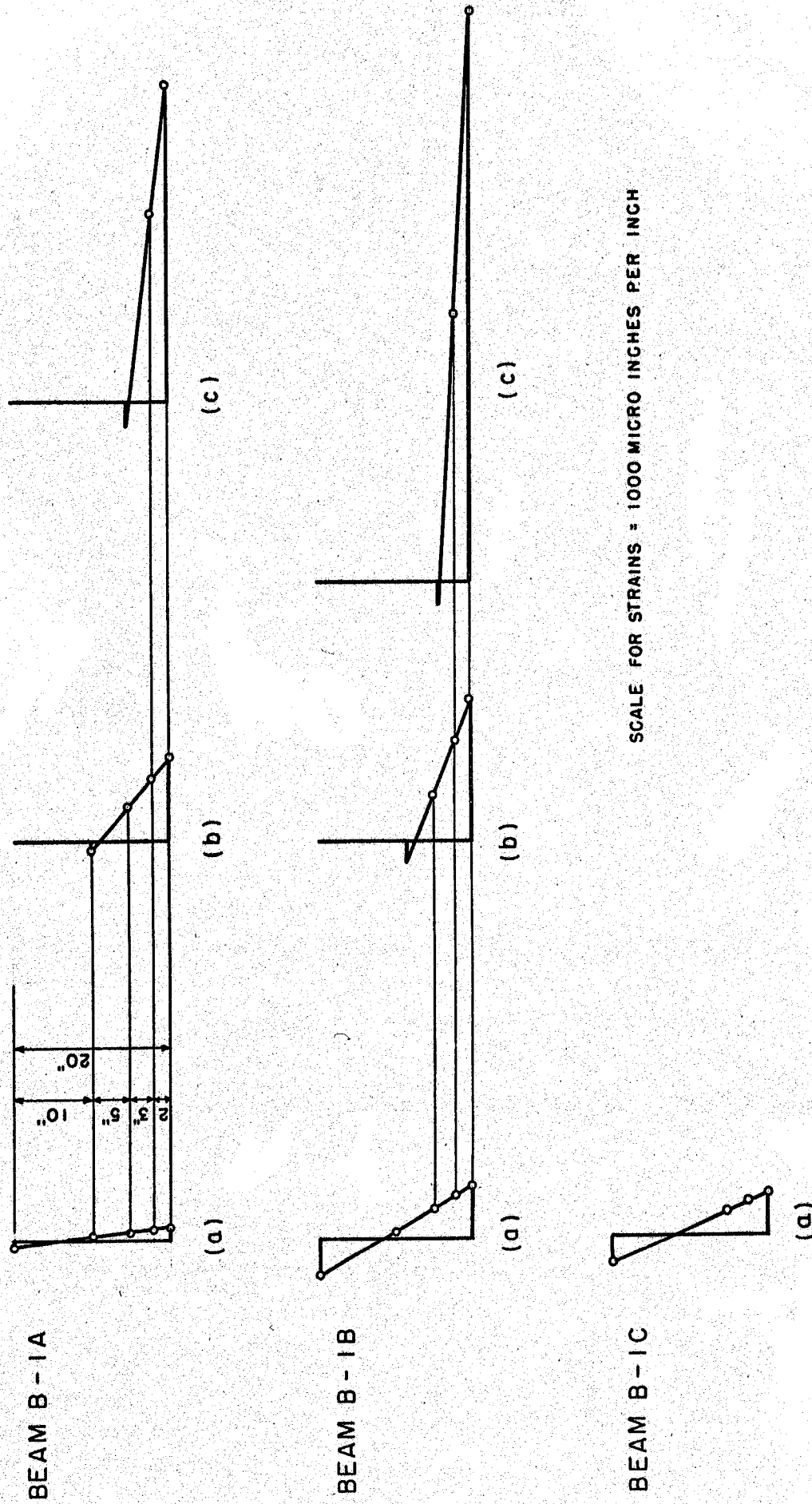


FIG.10 EXPERIMENTAL STRAIN DISTRIBUTIONS  
 (a) PRIOR TO CRACKING (b) AFTER CRACKING (c) AT ULTIMATE

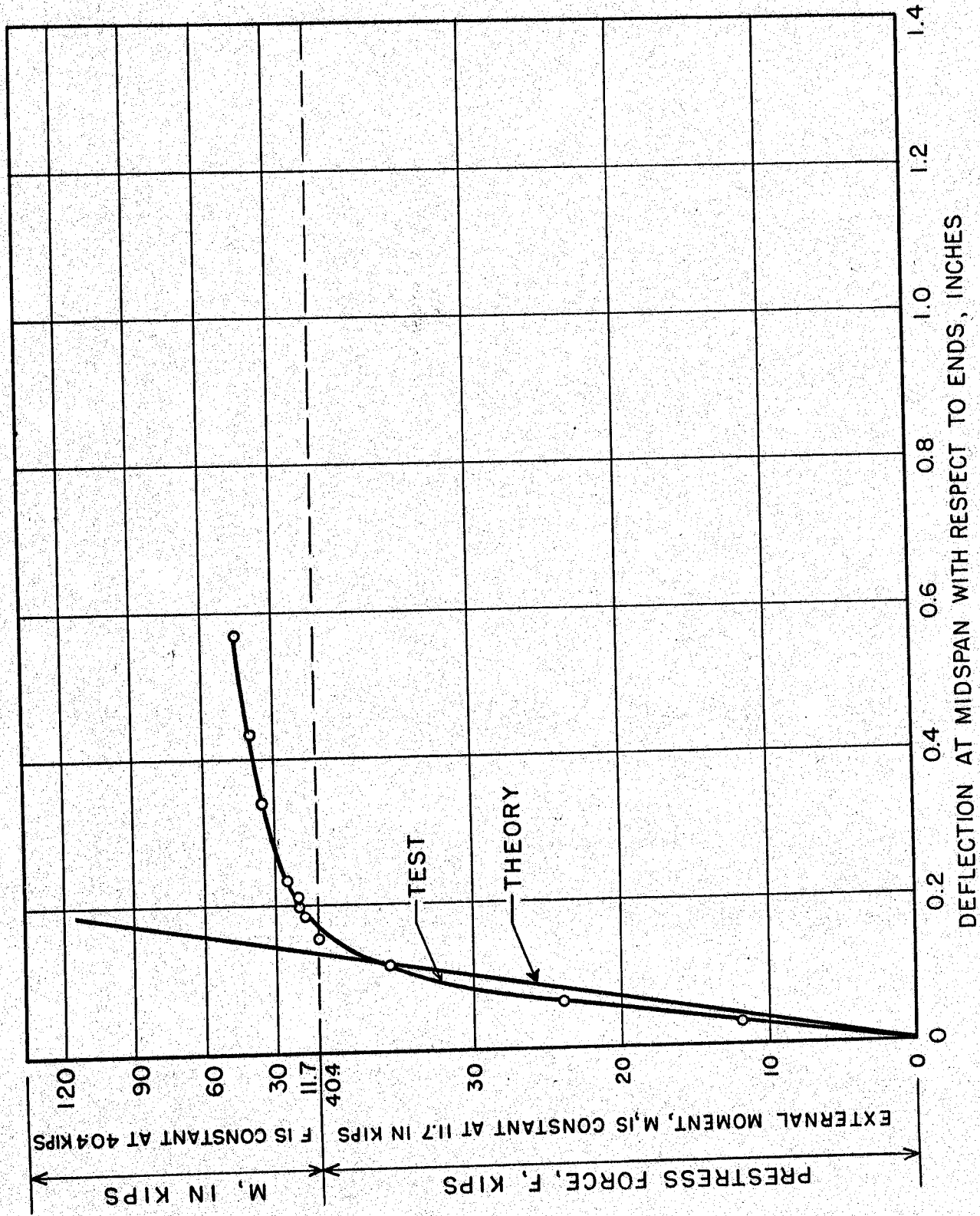


FIG. II BEAM B-1A; PRESTRESS FORCE AND MOMENT vs CENTER DEFLECTION

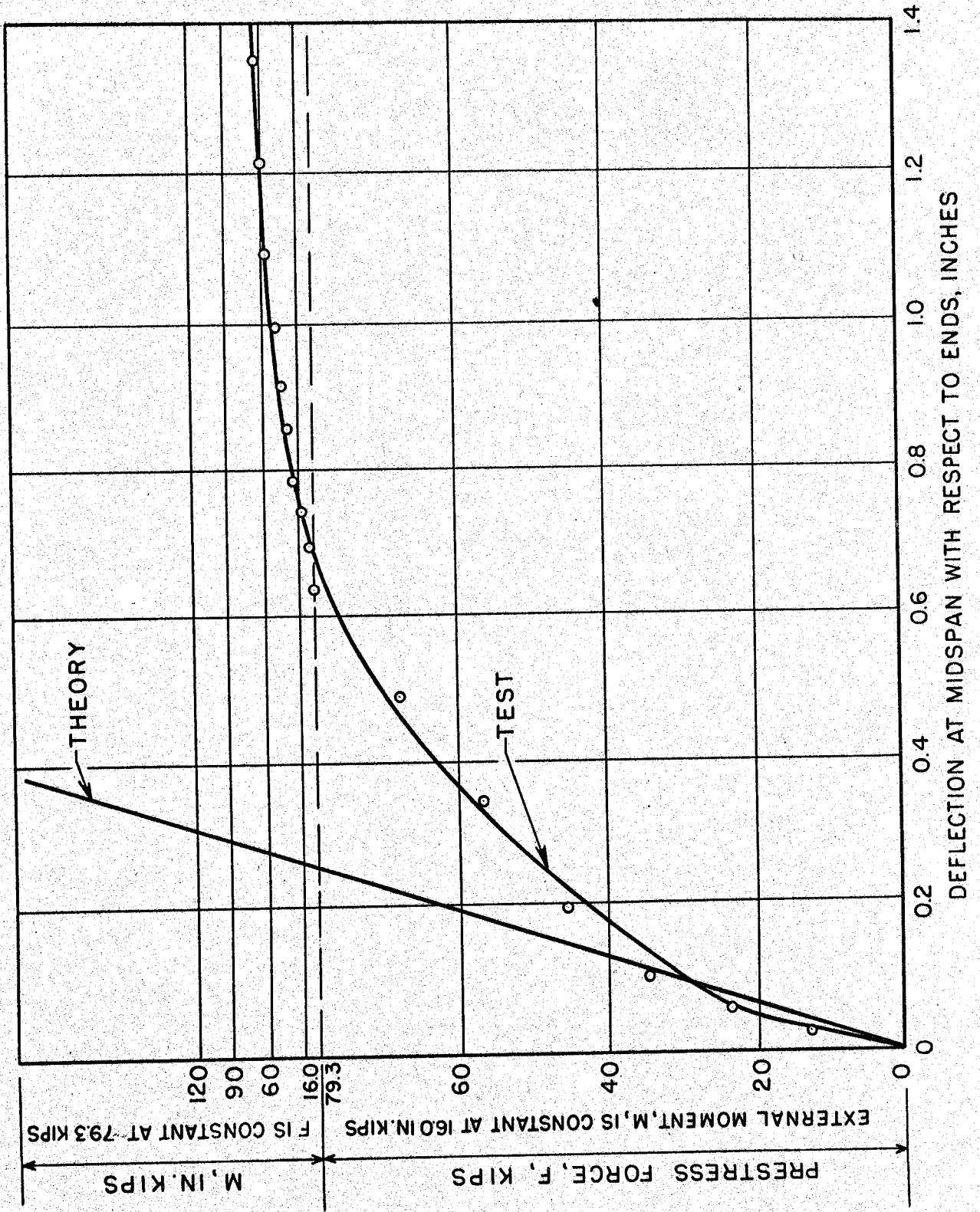


FIG.12 BEAM B-1B; PRESTRESS FORCE AND MOMENT vs CENTER DEFLECTION

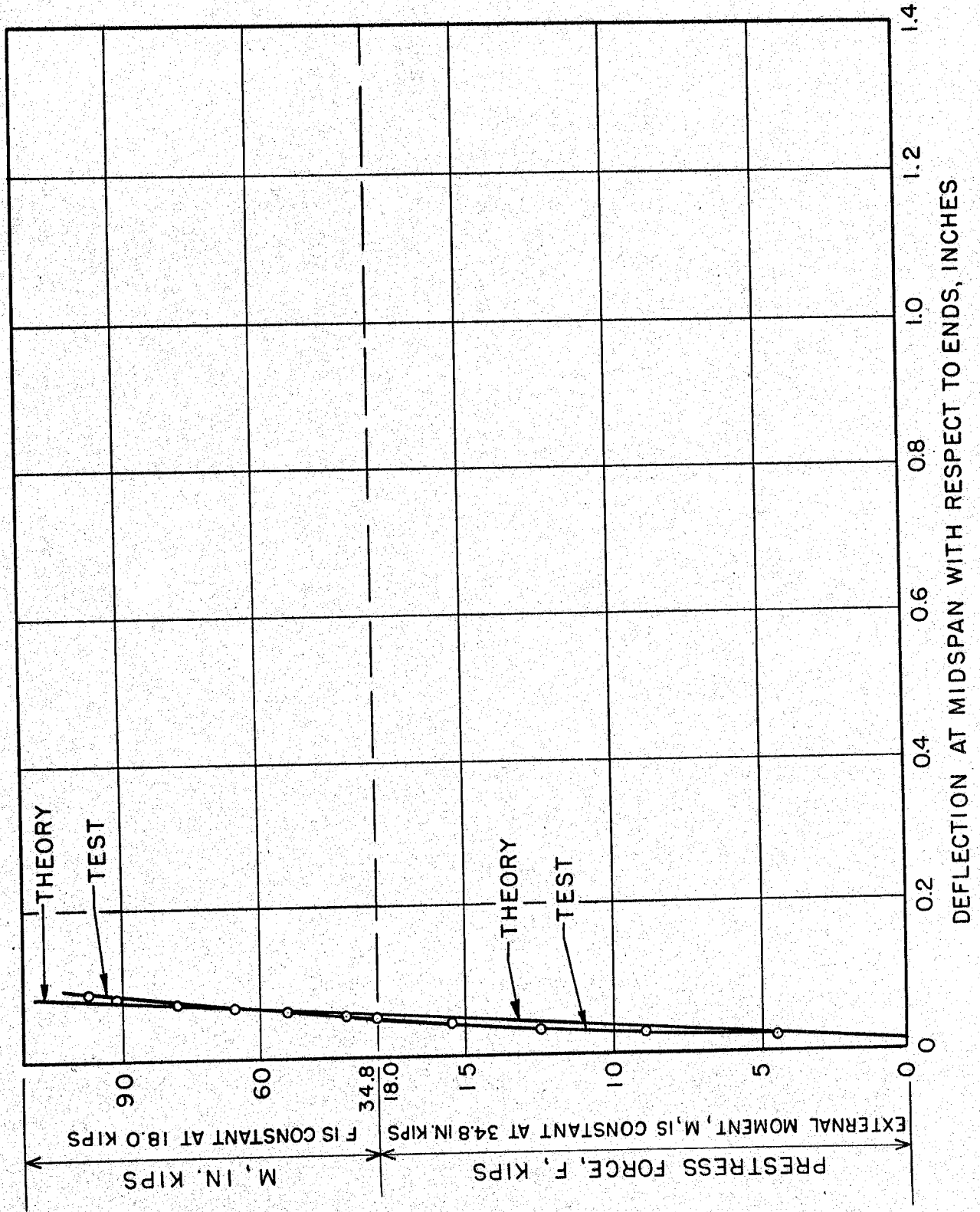
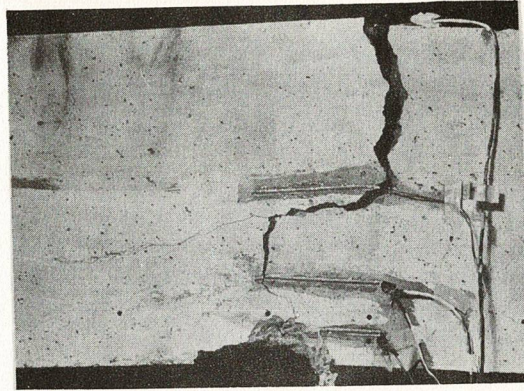
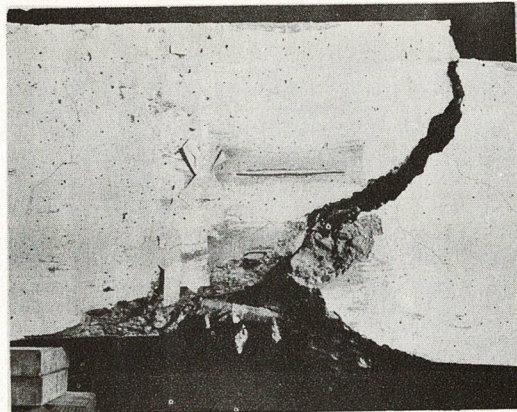


FIG. 13 BEAM B-1C; PRESTRESS FORCE AND MOMENT vs CENTER DEFLECTION

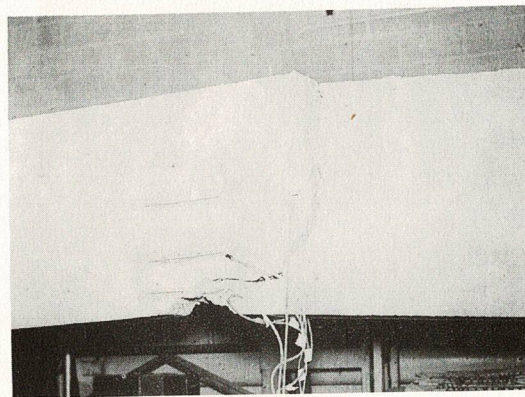




BEAM B - 1A



BEAM B - 1B



BEAM B - 1C

FIG. 14 BEAM SPECIMENS AFTER FAILURE